

Soft and semihard components of multiplicity distributions in the k_T factorization approach

H. R. Martins-Fontes* and F. S. Navarra†

*Instituto de Física, Universidade de São Paulo, Rua do Matão 1371,
Cidade Universitária, - 05508-090, São Paulo, SP, Brazil.*

(Dated: June 23, 2025)

Particle production in hadronic collisions can be studied in the low-momentum (soft) and high-momentum (hard) transfer regimes. While the latter can be well understood within perturbative QCD the former contains non-perturbative effects which cannot be calculated from first principles. There is also an intermediate regime called semihard, in which the momentum transfer runs typically from 1 to 10 GeV. As the hadron-hadron collision energy increases, we expect to see a relative growth of the number of semihard events. It has been conjectured that this growth would be the cause of some changes observed in the multiplicity distributions measured in proton - proton collisions. In this note we revisit the separation between soft and semihard events using the formalism of k_T factorization. The separation is implemented through the introduction of a scale that is the cutoff Λ in the transverse momentum of the produced gluon and allows us to compute the average number of particles produced in each regime. These numbers are used as input in the double negative binomial fit of data, from which we can extract correlations between the fraction of semihard events and the violation of KNO scaling.

* henriquemartinsfontes@usp.br

† navarra@if.usp.br

I. INTRODUCTION

The multiplicity distribution (MD) of charged particles measured in high energy proton-proton collisions is one of the observables that is not yet well understood in QCD. For a comprehensive review, see [1]. For the multiplicities of particles in jets, in the limit of very high energies and very high multiplicities, there are robust predictions of perturbative QCD (pQCD) [2]. For other types of events, there are significant non-perturbative effects and we cannot perform calculations from first principles. In the absence of a straightforward connection between theory and data, we have to resort to models. However even this task is complex because of the non-perturbative nature of hadronization. The "top-down" models, such as those based on the Color Glass Condensate (CGC) [3] approach, or event generators, such as PYTHIA [4, 5], give only an approximate description of the measured MD's which exhibit a complex structure. Many works have taken a "bottom-up" approach, i.e. trying first to find empirical regularities in the data, obtaining successful parametrizations of these data and then searching for scaling laws and their violation. After this first step, one tries to connect the empirical observations with the theory. Along this line the fits with the Negative Binomial Distribution (NBD) were very successful for many years and specially for lower energies data. But, at the $\sqrt{s} = 900$ GeV SPS energy, the NBD started to fail in describing the measured multiplicity distributions, which exhibited a shoulder-shaped structure [1].

For LHC energies, a single NBD fit turned out to be problematic. In the early ALICE data [6], for the class of non-single diffractive (NSD) events, no strong deviation from a single NBD fit was observed at $\sqrt{s} = 0.9$ and 2.36 TeV for $|\eta| < 1$, but a hint of a substructure appeared at $|\eta| < 1.3$. However, in [7] for all event classes, already at $\sqrt{s} = 0.9$ TeV, the single NBD fits started to diverge from the data at the highest multiplicities for $|\eta| < 0.5$ and 1.0. Even more significant departures from the single NBD started at $\sqrt{s} = 2.76$ TeV.

A fruitful idea was to interpret the shoulder-like structure observed in the data as coming from a superposition of two negative binomial distributions (called DNBD). The two NBDs could be associated to two different sources or two different types of processes. In the first case, as advocated, for example, in [8, 9], the sources are well separated in rapidity. In the second case, the two NBDs would come from soft and semihard processes. This latter idea was advanced long ago in [10], further developed in [11] and more recently in [12]. A review on this subject can be found in [13]. For the TeV region, the expectation was that at increasing energies the semihard component would become increasingly more important than the soft one. In parallel, a violation of the Koba-Nielsen-Olsen (KNO) scaling [14] was observed, suggesting a connection between the two findings. The latest LHC data [15, 16] confirmed that for narrow pseudorapidity windows a single NBD was enough to reproduce the observed distributions and also that KNO scaling was valid. For larger windows, two NBDs were needed and KNO scaling was violated.

In [11, 13] the difference between soft and semihard processes was only that the latter yield larger mean multiplicities. In the present work, using the k_T factorization formalism [17, 18], we can make a better separation with the proper introduction of an energy scale. Moreover, the introduction of this formalism reduces the number of parameters. As will be seen, we will obtain fits with very good quality and we will extract from them, with less ambiguity, the behavior of the parameter α with the energy \sqrt{s} and with the size of the pseudorapidity window. This parameter represents the fraction of soft events.

II. THE k_T FACTORIZATION APPROACH

At high energy collisions between hadrons or heavy ions, a large number of gluons is produced due to the dense gluon population in the hadron wave function. Using the CGC formalism, particle production in high-energy hadronic collisions can be studied through the k_T factorization approach, where the inclusive production cross-section is given by [18, 19]:

$$E \frac{d\sigma}{d^3p} = K \frac{4\pi N_c}{N_c^2 - 1} \alpha_s(Q^2) \frac{1}{p_\perp^2} \int^{p_\perp} dk_\perp^2 \varphi_1(x_1, k_\perp^2) \varphi_2(x_2, (p - k)_\perp^2), \quad (1)$$

where $x_{1,2} = \frac{p_\perp}{\sqrt{s}} \exp(\pm y)$, \sqrt{s} is the center of mass energy, N_c is the number of colors and K is a normalization factor that describes the conversion of partons to hadrons. φ is the unintegrated gluon distribution (UGD) of a proton and it can be related to the gluon density by

$$xG(x, \mu^2) = \int^{\mu^2} dk_\perp^2 \varphi(x, k_\perp^2). \quad (2)$$

The multiplicity per unit of rapidity can be computed by integrating (1) over p_\perp

$$\frac{dN}{dy} = \frac{1}{S} \int_{p_{\perp min}}^{p_{\perp max}} d^2p_\perp E \frac{d\sigma}{d^3p}, \quad (3)$$

where S is a typical interaction area and the minimum and maximum value of p_\perp are determined by the experimental conditions. In (3), the main contribution is given by two regions of integration over k_\perp : $k_\perp \ll p_\perp$ and $|p_\perp - k_\perp| \ll p_\perp$. Hence we can rewrite it as [20]:

$$\begin{aligned} \frac{dN}{dy} &= \frac{K}{S} \frac{4\pi N_c}{N_c^2 - 1} \int_{p_{\perp min}}^{p_{\perp max}} \frac{dp_\perp^2}{p_\perp^2} \alpha_s(Q^2) \left[\varphi_1(x_1, p_\perp) \int^{p_\perp} dk_\perp^2 \varphi_2(x_2, k_\perp) + \varphi_2(x_2, p_\perp) \int^{p_\perp} dk_\perp^2 \varphi_1(x_1, k_\perp) \right] \\ &= \frac{K}{S} \frac{4\pi N_c}{N_c^2 - 1} \int_{p_{\perp min}}^{p_{\perp max}} \frac{dp_\perp^2}{p_\perp^4} \alpha_s(Q^2) x G_2(x_2, p_\perp^2) x G_1(x_1, p_\perp^2), \end{aligned} \quad (4)$$

where the equation in the first line was integrated by parts and use was made of (2). The multiplicative constants K and S can be grouped in a single parameter which is fixed by fitting the available pseudo-rapidity distributions. For the UGD, we adopt the one from the GBW model [21, 22] because it comes from a simple and well-established dipole parameterization, which it is known for its success in the description of a wealth of experimental data on particle production, including both hard and soft processes. For the purposes of our work the GBW model is specially appropriate because it reproduces very well the DIS data on F_2 at very low scales, which are consistent with the low transverse momenta of the bulk of produced particles at the LHC. At these scales the UGD derived from the GBW model is also consistent with much more sophisticated UGDs [23]. For a recent account of the successes of the GBW model, see [24] and references therein. The GBW UGD reads:

$$\varphi_{1,2}(x_{1,2}; k_\perp^2) = \frac{3\sigma_0}{4\pi^2 \alpha_s(Q_{s1,2}^2)} \frac{k_\perp^2}{Q_{s1,2}^2} \exp\left(-\frac{k_\perp^2}{Q_{s1,2}^2}\right), \quad (5)$$

where the saturation scale Q_s^2 is defined as

$$Q_{s1,2}^2 = Q_0^2 \left(x_0 \frac{\sqrt{s}}{Q_0} e^{\pm y} \right)^{\bar{\lambda}}. \quad (6)$$

The parameters were fixed as in [19]: $Q_0 = 0.6$ GeV, $x_0 = 0.01$, $\bar{\lambda} = 0.205$, and $\sigma_0 = 23$ mb. The running coupling constant α_s follows the one-loop approximation and is assumed to freeze at 0.52:

$$\alpha_s(Q^2) = \min \left[\frac{12\pi}{27 \ln \left(\frac{Q^2}{\Lambda_{QCD}^2} \right)}, 0.52 \right], \quad (7)$$

with $\Lambda_{QCD} = 0.226$ GeV. The scale Q^2 at which the strong coupling $\alpha_s(Q^2)$ is evaluated in Eq. (4) is defined as

$$Q^2 = \max[p_\perp^2, \min(Q_{s1}^2, Q_{s2}^2)]. \quad (8)$$

The UGD (5) leads to the gluon distribution function expressed as

$$x G_{1,2}(x_{1,2}; p_\perp^2) = \frac{3\sigma_0}{4\pi^2 \alpha_s(Q_{s1,2}^2)} \left(Q_{s1,2}^2 - \exp\left(-\frac{p_\perp^2}{Q_{s1,2}^2}\right) (p_\perp^2 + Q_{s1,2}^2) \right) (1 - x_{1,2})^4. \quad (9)$$

Here, as in [20], the factor $(1 - x)^4$ is introduced to account for large- x effects. In expression Eq. (1), and also in Eq. (4), one gluon with p_\perp is produced from the fusion of a gluon with k_\perp and another gluon with $p_\perp - k_\perp$. Therefore the momentum p_\perp is, to a good approximation, the minimum value of the momentum flowing in the three gluon vertex, i.e. the one to be used in the running coupling constant. For p_\perp larger than a few GeV, the coupling $\alpha_s(Q^2)$ becomes sufficiently smaller than one and we are in the perturbative domain. We will thus follow the literature and call these events "semihard". The events with lower values of p_\perp will be called "soft". Accordingly the total multiplicity per unit of rapidity is the sum of the contributions from the soft and semihard events. The separation is achieved by introducing a cutoff Λ in the integral over p_\perp , which defines the two contributions:

$$\begin{aligned} \frac{dN}{dy} &= \frac{K}{S} \frac{4\pi N_c}{N_c^2 - 1} \left[\int_{p_{\perp min}}^{\Lambda} \frac{dp_\perp^2}{p_\perp^4} \alpha_s(Q^2) x G_2(x_2, p_\perp^2) x G_1(x_1, p_\perp^2) + \int_{\Lambda}^{p_{\perp max}} \frac{dp_\perp^2}{p_\perp^4} \alpha_s(Q^2) x G_2(x_2, p_\perp^2) x G_1(x_1, p_\perp^2) \right] \\ &= \frac{dN_s}{dy} + \frac{dN_{sh}}{dy}. \end{aligned} \quad (10)$$

where N_s and N_{sh} are the soft and semihard components respectively. In the context of the CGC formalism, a similar separation criterion was introduced in [25]. To calculate the pseudo-rapidity distributions, one should rewrite expression (10) using the transformation

$$y(\eta) = \frac{1}{2} \log \frac{\sqrt{\cosh^2 \eta + \mu^2} + \sinh \eta}{\sqrt{\cosh^2 \eta + \mu^2} - \sinh \eta}, \quad (11)$$

where the scale μ is given as [26]

$$\mu(\sqrt{s}) = \frac{0.24}{0.13 + 0.32 (\sqrt{s})^{0.115}}. \quad (12)$$

and the Jacobian reads:

$$J(\eta) = \frac{\partial y}{\partial \eta} = \frac{\cosh \eta}{\sqrt{\cosh^2 \eta + \mu^2}}, \quad (13)$$

Changing variables and integrating (10) over the pseudo-rapidity we obtain the average multiplicity:

$$N = N_s + N_{sh}. \quad (14)$$

We emphasize that the only free parameter is the constant K/S which is going to be determined by using Eq. (10) to fit the measured pseudo-rapidity distributions. It is also important to mention that Eq. (10) describes the gluon production and, after integration, the number of gluons produced. As done in previous works, we shall assume here that the number of produced partons is equal to the number of hadrons resulting from the hadronization of these partons ("parton-hadron duality"). The approximate equality between these numbers has been (successfully) tested recently in [27], where the authors used PYTHIA to calculate the hadron multiplicities within jets with and without using the LUND prescription for hadronization. They found a small difference between the number of partons and the number of hadrons.

In Fig. 1 we show the rapidity distributions measured by different collaborations of the LHC at different energies. The k_T factorization distribution seems to be consistent with the data, and thus we believe that for the purposes of this work, using Eq. (10) is sufficient.

III. DOUBLE NEGATIVE BINOMIAL DISTRIBUTION

In [28] Giovannini e Ugoccioni proposed a two-component model combining two NBDs associated with two event classes: "soft" and "semihard" processes. Recent analyses performed by the ALICE Collaboration showed that the double NBD fit yields a good description of the data on multiplicity distributions from 0.9 to 8 TeV [7, 15, 29] within several pseudo-rapidity windows. In this work, we will use their model. The DNBD is expressed as:

$$P(n) = \lambda [\alpha P(n, \langle n \rangle_s, k_s) + (1 - \alpha) P(n, \langle n \rangle_{sh}, k_{sh})], \quad (15)$$

where

$$P(n, \langle n \rangle, k) = \frac{\Gamma(k+n)}{\Gamma(k)\Gamma(n+1)} \frac{\langle n \rangle^n k^k}{(\langle n \rangle + k)^{n+k}}. \quad (16)$$

and where, in each NBD, $\langle n \rangle$ is the average multiplicity and the parameter k is related to the dispersion D ($D^2 = \langle n^2 \rangle - \langle n \rangle^2$) through:

$$\frac{D_i^2}{\langle n \rangle_i^2} = \frac{1}{\langle n \rangle_i} + \frac{1}{k_i}, \quad (17)$$

where $i = \{s, sh\}$. The parameter α is the fraction of soft events and consequently $(1 - \alpha)$ is the fraction of semihard events; $\langle n \rangle_s$ and $\langle n \rangle_{sh}$ are the mean multiplicities of soft and semihard events respectively; k_s and k_{sh} are the negative binomial parameters of the soft and semihard components. The first few bins can not be reproduced by any NBD and they are related to a different production mechanism, not included in our formalism. Therefore, these bins were removed from the fitting process. To account for this, a normalization factor λ was introduced [7, 29]. The average multiplicity obtained from (15) can be expressed as:

$$\langle n \rangle = \lambda [\alpha \langle n \rangle_s + (1 - \alpha) \langle n \rangle_{sh}]. \quad (18)$$

Comparing expression (18) with (14) and recalling that $N = \langle n \rangle$ we conclude that:

$$\begin{aligned}\lambda \alpha \langle n \rangle_s &= N_s \\ \lambda (1 - \alpha) \langle n \rangle_{sh} &= N_{sh}\end{aligned}\tag{19}$$

Since N_s and N_{sh} are known, these two equations reduce the number of free parameters from six to four: α , λ , k_s , and k_{sh} .

IV. KNO SCALING

The Koba-Nielsen-Olesen (KNO) scaling [14] is a feature of MDs that asserts that, in the limit of $\langle n \rangle \rightarrow \infty$, the probability distributions $P(n)$ at different energies, once rescaled by $\langle n \rangle$, become copies of each other. In other words, if one plots $\langle n \rangle P(n)$ versus $n/\langle n \rangle$ for different energies, all curves collapse onto a universal function $\psi(n/\langle n \rangle)$:

$$\langle n \rangle P(n) = \psi\left(\frac{n}{\langle n \rangle}\right).\tag{20}$$

A direct consequence of the KNO scaling is that the total scaled variance, in the scaling limit, increases linearly with $\langle n \rangle$ [30–32]

$$\omega = \frac{D^2}{\langle n \rangle} = \kappa \langle n \rangle,\tag{21}$$

with $\kappa = \text{const} > 0$. In the case of the DNBD, using (18) we have:

$$\begin{aligned}D^2 &= \lambda [\alpha \langle n^2 \rangle_s + (1 - \alpha) \langle n^2 \rangle_{sh}] - \langle n \rangle^2 = \lambda [\alpha (D_s^2 + \langle n \rangle_s^2) + (1 - \alpha) (D_{sh}^2 + \langle n \rangle_{sh}^2)] - \langle n \rangle^2 \\ &= \lambda \left[\alpha \left(\langle n \rangle_s + \frac{\langle n \rangle_s^2}{k_s} + \langle n \rangle_s^2 \right) + (1 - \alpha) \left(\langle n \rangle_{sh} + \frac{\langle n \rangle_{sh}^2}{k_{sh}} + \langle n \rangle_{sh}^2 \right) \right] - \langle n \rangle^2 \\ &= \langle n \rangle - \langle n \rangle^2 + \lambda \left[\alpha \langle n \rangle_s^2 \left(1 + \frac{1}{k_s} \right) + (1 - \alpha) \langle n \rangle_{sh}^2 \left(1 + \frac{1}{k_{sh}} \right) \right]\end{aligned}\tag{22}$$

where in the second line we made use of (17). Dividing the above equation by $\langle n \rangle$ we obtain the scaled variance:

$$\omega = \frac{D^2}{\langle n \rangle} = 1 - \langle n \rangle + \frac{\langle n \rangle}{\langle n \rangle^2} \lambda \left[\alpha \langle n \rangle_s^2 \left(1 + \frac{1}{k_s} \right) + (1 - \alpha) \langle n \rangle_{sh}^2 \left(1 + \frac{1}{k_{sh}} \right) \right]\tag{23}$$

and hence

$$\omega = 1 + \frac{1}{k_{total}} \langle n \rangle,\tag{24}$$

where

$$\frac{1}{k_{total}} = \frac{\lambda \alpha \langle n \rangle_s^2 \left(1 + \frac{1}{k_s} \right) + \lambda (1 - \alpha) \langle n \rangle_{sh}^2 \left(1 + \frac{1}{k_{sh}} \right)}{\langle n \rangle^2} - 1.\tag{25}$$

In the limit $\langle n \rangle \rightarrow \infty$, we finally obtain:

$$\omega \approx \frac{1}{k_{total}} \langle n \rangle.\tag{26}$$

which is precisely (21) with $1/k_{total}$ being the positive constant. Hence the validity of KNO scaling requires that $1/k_{total}$ remains energy independent and in our analysis of data we will look at this quantity.

It is possible to improve the quantitative study KNO scaling by analyzing the energy dependence of the C-moments ($C_q = \langle n^q \rangle / \langle n \rangle^q$). In the limit $\langle n \rangle \rightarrow \infty$ they should become energy independent. In the case of single NBD models one can derive analytic expressions for the C_q moments as a function of $\langle n \rangle$. In [33] it was shown that

$$C_2 = \frac{1}{\langle n \rangle} + 1 + \frac{1}{k}$$

In the large mean multiplicity (and hence energy) limit C_2 is constant if k is constant. In [33] it was shown that when $|\eta| < 0.5$ this is approximately the case and C_2 is constant. For larger pseudorapidity windows, this is no longer true. The higher moments show a more complicated dependence on $\langle n \rangle$ and the data show larger error bars. We will not perform the study of the moments in this work. Nevertheless, we would like to point out that for the double NBD approach it is possible to establish a connection between the moments and k_{total} . For example, it is easy to show that in the scaling limit we have

$$C_2 = \frac{1}{k_{total}}$$

Before closing this section, we would like to mention that studying KNO scaling belongs to the "bottom-up" approaches to multiplicity distributions mentioned in the Introduction and it is not the only scaling that has been investigated. Other empirical regularities have been found in the data, which might have consequences for the multiplicity distributions, such as geometric scaling [23] (and references therein) and entropy scaling [34].

V. RESULTS AND DISCUSSION

The global normalization parameter K/S is obtained by fitting Eq. (10) to the data at different energies. The values of K/S are shown in Table I. It is reassuring to see that this normalization factor depends very weakly on the energy. As can be seen in Fig. 1, we obtain an overall good description of the pseudorapidity distribution data.

data	\sqrt{s} (TeV)	K/S (GeV ²)
[35]	0.9	0.0968 ± 0.0011
[7]	0.9	0.1015 ± 0.0011
[35]	2.36	0.0993 ± 0.0011
[7]	2.76	0.1001 ± 0.0012
[16]	5.02	0.0929 ± 0.0005
[36]	7.0	0.0975 ± 0.0012
[7]	7.0	0.0965 ± 0.0007
[7]	8.0	0.0952 ± 0.0007
[16]	13.0	0.0888 ± 0.0005

TABLE I: Values of K/S for different energies. The data used for the fits are from CMS [35, 36] and ALICE [7, 16].

To obtain the soft and semihard average multiplicities from (10) we will fix the separation scale to be $\Lambda = 1.4$ GeV. This is approximately the same number used in [37] and is in the range of usual values used to define the separation between soft and semihard physics (see [38] and [37] for further references). Having fixed these numbers, we use equation (19) together with (15) to perform a fit of all the LHC data on MDs in order to determine the parameters λ , α , k_s and k_{sh} . The values of these parameters can be found in Table II in the Appendix, together with the values obtained for the multiplicities and for k_{total} .

From Table II we can infer that the variables which are usually called $\langle n_1 \rangle$ and $\langle n_2 \rangle$ indeed correspond to $\langle n_s \rangle$ and $\langle n_{sh} \rangle$ respectively. Moreover the previously found relation $\langle n_2 \rangle \simeq 3\langle n_1 \rangle$ becomes $\langle n_{sh} \rangle \simeq 3\langle n_s \rangle$ and is still valid, changing slightly with the center-of-mass energy and with the size of the rapidity window. This is consistent with the findings of the ALICE study published in [7] and in the analysis of CMS data performed in [11].

In Fig. 2, we show the comparison between the data and our model. We obtain fits of very good quality, which is reflected in the low values of χ^2 , among the smallest values reported in the literature for this class of model. The DNBD function provides a precise description of the entire set of multiplicity distributions measured at the LHC. This result is particularly remarkable given the reduction of free parameters from 6 to 4.

In order to verify whether KNO scaling is observed in the LHC data, we could simply plot the data. However, this would produce some visually cumbersome figures, specially when including the errors. Instead, since our fit of the data is very good, we plot the multiplicity distributions computed with Eq. (15) and presented in terms of the KNO variable. The resulting curves are shown in Fig. 3. It is very clear that for the smallest pseudorapidity window ($|\eta_c| < 0.5$) KNO scaling holds. For the others, the larger the window, the more KNO scaling is violated. In [2] it was shown that in the very high energy limit pQCD predicts scaling. Having this in mind, we might think that the perturbative events are concentrated in the narrow, central rapidity window and are responsible for the scaling, whereas the nonperturbative events are increasingly important at larger rapidity windows. If this were the case, we would expect that the parameter α would fall strongly with the energy for $|\eta_c| < 0.5$ and stay constant or increase in the other windows. However, this is not the case. In Fig. 4a we show the behavior of α with \sqrt{s} for all windows

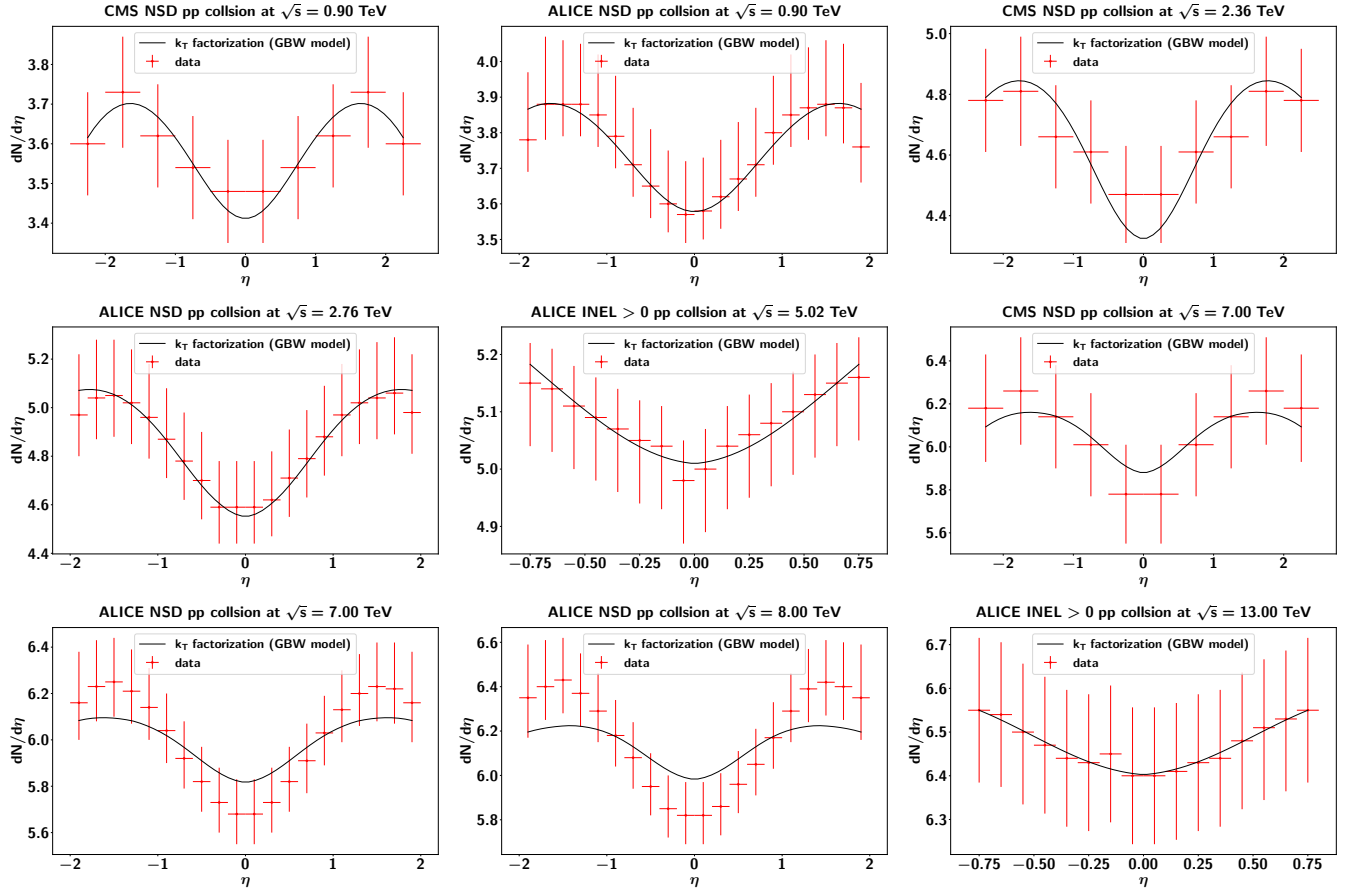


FIG. 1: Pseudorapidity distributions. The solid lines are obtained from Eq. (10). Data are from CMS [35, 36] and ALICE [7, 16]; the bars show the combined uncertainties.

multiplied by some numerical factor for the sake of clarity. We can see that the falling behavior is the same for all windows and, contrary to previous expectations, there is no correlation between α and the violation of KNO scaling. In fact, if we did not multiply the values of α by the separating numerical factors, they would fall onto a single curve (within a few percent of uncertainty). Interestingly, in [7] the ALICE Collaboration performing a similar DNBD analysis of the same data found that α increases with the energy \sqrt{s} in all rapidity windows (see Table 10 in that reference). This is an example of how the introduction of constraints can bring about not only quantitative but also qualitative changes in the behavior of the fit parameters.

As for the other parameters, we see a marked change in the behavior of k_s and k_{sh} with \sqrt{s} , going from constant when $|\eta_c| < 0.5$ to rapidly falling when $|\eta_c| > 1.0$, as can be seen in Figs. 4b and 4c. Giovannini and Ugoccioni proposed in [10, 40] three scenarios for the behavior of k_s and k_{sh} :

- i) Both k_s and k_{sh} remain constant with energy, which means that KNO scaling is valid for both soft and semi-hard components.
- ii) k_s is constant with energy and k_{sh} decreases linearly with increasing energy, implying that KNO scaling is strongly violated by the semihard component.
- iii) k_s is constant with energy and k_{sh} starts decreasing with increasing energy, but asymptotically tends to a constant value, implying that KNO scaling violation is not very strong.

Our results suggest that none of these scenarios is supported by data. Moreover we emphasize the importance of the relation (26) and of studying the behavior of k_{total} . Indeed, since λ and α may depend on the energy, the simple constancy of k_s and k_{sh} does not ensure KNO scaling. The constancy of k_{total} does. In Fig. 4d we show k_{total} as a function of the energy for different pseudorapidity windows. It is constant for $|\eta| < 1.0$ and energy-dependent for $|\eta| > 1.0$.

We can compare our results with those found in [7] where a similar DNBD fit was performed. The comparison shows that the order of magnitude of the parameters is the same. However, in contrast to [7], we find a clear trend

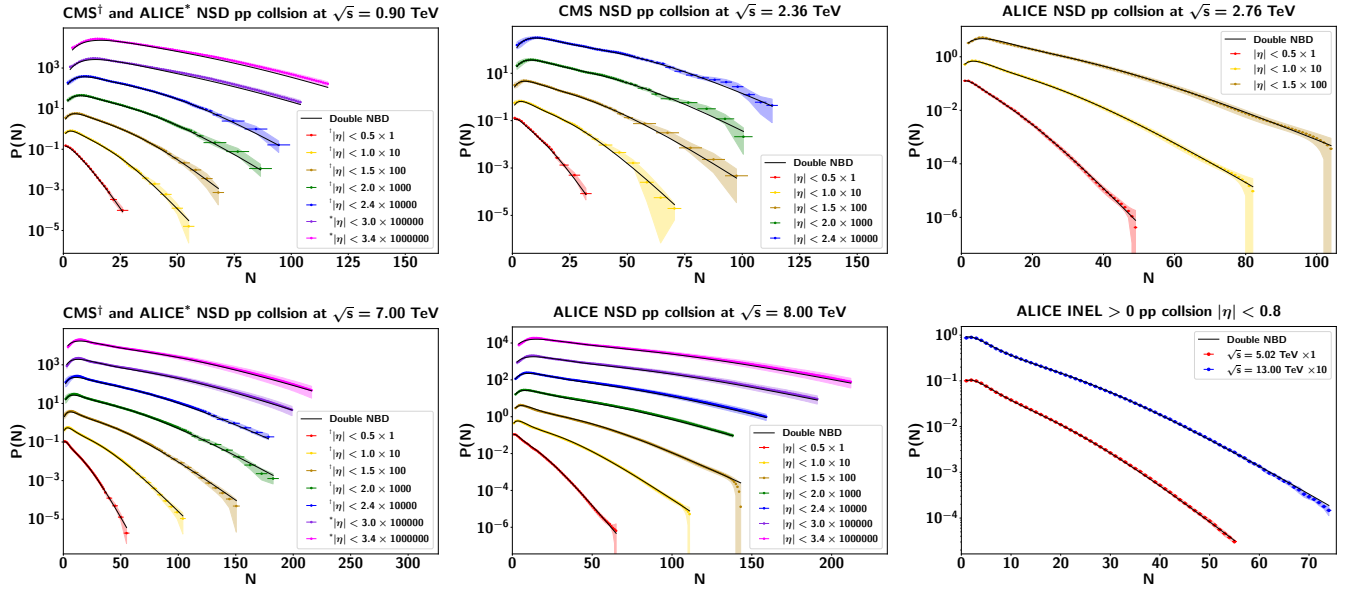


FIG. 2: Multiplicity distributions measured by different collaborations. In the bottom-right panel we show the MDs measured in inelastic events (INEL). All the other panels show data from non-single-diffractive (NSD) events. The fits are obtained with Eq. (15) and the fit parameters are listed in Table II. Data are from CMS [39] and ALICE [7, 15, 29]. The colored bands show the combined uncertainties.

which separates the narrower rapidity windows, $|\eta| < 1.0$, from the wider ones, with $|\eta| > 1.0$. In the former k_s and k_{sh} are constant with energy, whereas in the latter these parameters decrease with increasing energies. This feature and the fact that in the narrower window we observe KNO scaling and not in the others strongly suggest that there is a change of dynamics when we go from one region to the other.

To summarize:

1. Using the k_T factorization formalism and introducing a separation scale in the transverse momentum we were able to properly define soft and semihard multiplicities, giving a physical meaning to the previously called multiplicity components n_1 and n_2 , proposed in [28] and used in [7, 15, 29].
2. With this separation, we could perform a DNBD fit of the multiplicity distributions measured at the LHC with fewer free parameters (4 instead of 6), obtaining very good fits.
3. The resulting behavior of the parameters α , k_s and k_{sh} with the collision energy is consistent (but slightly different) with those found in previous analyses.
4. KNO scaling occurs for the total MD when k_{total} is independent of the \sqrt{s} and this happens only for $|\eta| < 1.0$. Furthermore, within the same pseudorapidity window, KNO scaling is also satisfied for the soft and semihard components; that is, k_s and k_{sh} are also energy independent.
5. KNO violation is not related to changes in α and may have a dynamical origin due to changes in N_s , N_{sh} , k_s and k_{sh} with pseudorapidity.

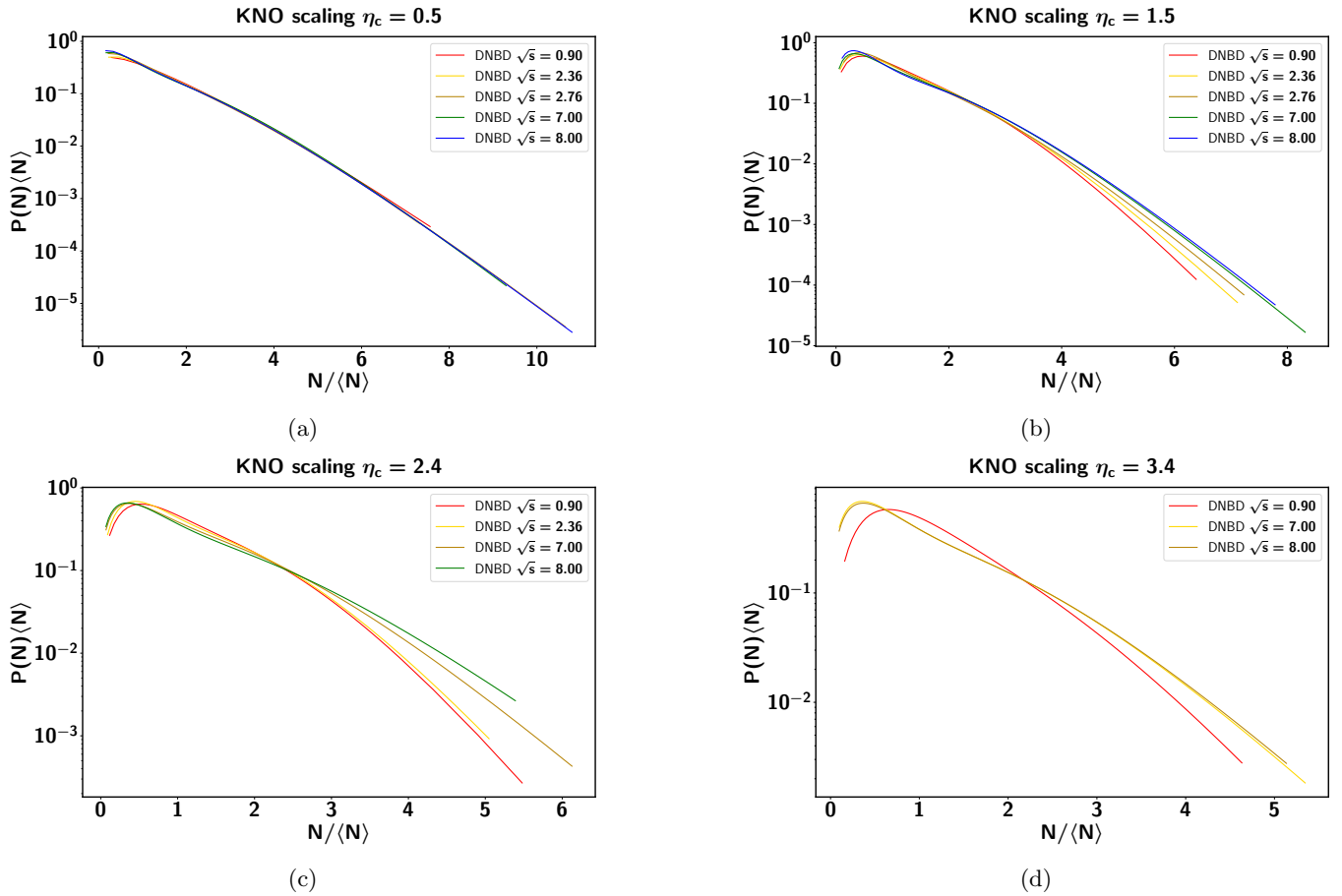


FIG. 3: KNO scaling of multiplicity distributions for various pseudorapidity windows ($-\eta_c < \eta < +\eta_c$).

ACKNOWLEDGMENTS

We are grateful to M. Munhoz, G. Wilk and M.V.T. Machado for useful discussions. We were supported by the Brazilian funding agencies CAPES, FAPESP, CNPq and INCT-FNA.

Appendix A: Tables

-
- [1] J. F. Grosse-Oetringhaus and K. Reygers, J. Phys. G **37**, 083001 (2010); [arXiv:0912.0023 [hep-ex]].
 - [2] Y. L. Dokshitzer and B. R. Webber, [arXiv:2505.00652 [hep-ph]].
 - [3] F. Gelis, E. Iancu, J. Jalilian-Marian and R. Venugopalan, Ann. Rev. Nucl. Part. Sci. **60**, 463 (2010); [arXiv:1002.0333 [hep-ph]].
 - [4] T. Sjostrand, S. Mrenna and P. Z. Skands, JHEP **05**, 026 (2006); [arXiv:hep-ph/0603175 [hep-ph]].
 - [5] C. Bierlich, S. Chakraborty, G. Gustafson and L. Lönnblad, JHEP **03**, 270 (2021); [arXiv:2010.07595 [hep-ph]].
 - [6] K. Aamodt *et al.* [ALICE], Eur. Phys. J. C **68**, 89 (2010); [arXiv:1004.3034 [hep-ex]].
 - [7] J. Adam *et al.* [ALICE], Eur. Phys. J. C **77**, 33 (2017); [arXiv:1509.07541 [nucl-ex]].
 - [8] G. N. Fowler, F. S. Navarra, M. Plumer, A. Vourdas, R. M. Weiner and G. Wilk, Phys. Rev. C **40**, 1219 (1989).
 - [9] G. N. Fowler, E. M. Friedlander, R. M. Weiner and G. Wilk, Phys. Rev. Lett. **57**, 2119 (1986); [erratum: Phys. Rev. Lett. **57**, 3124 (1986)].

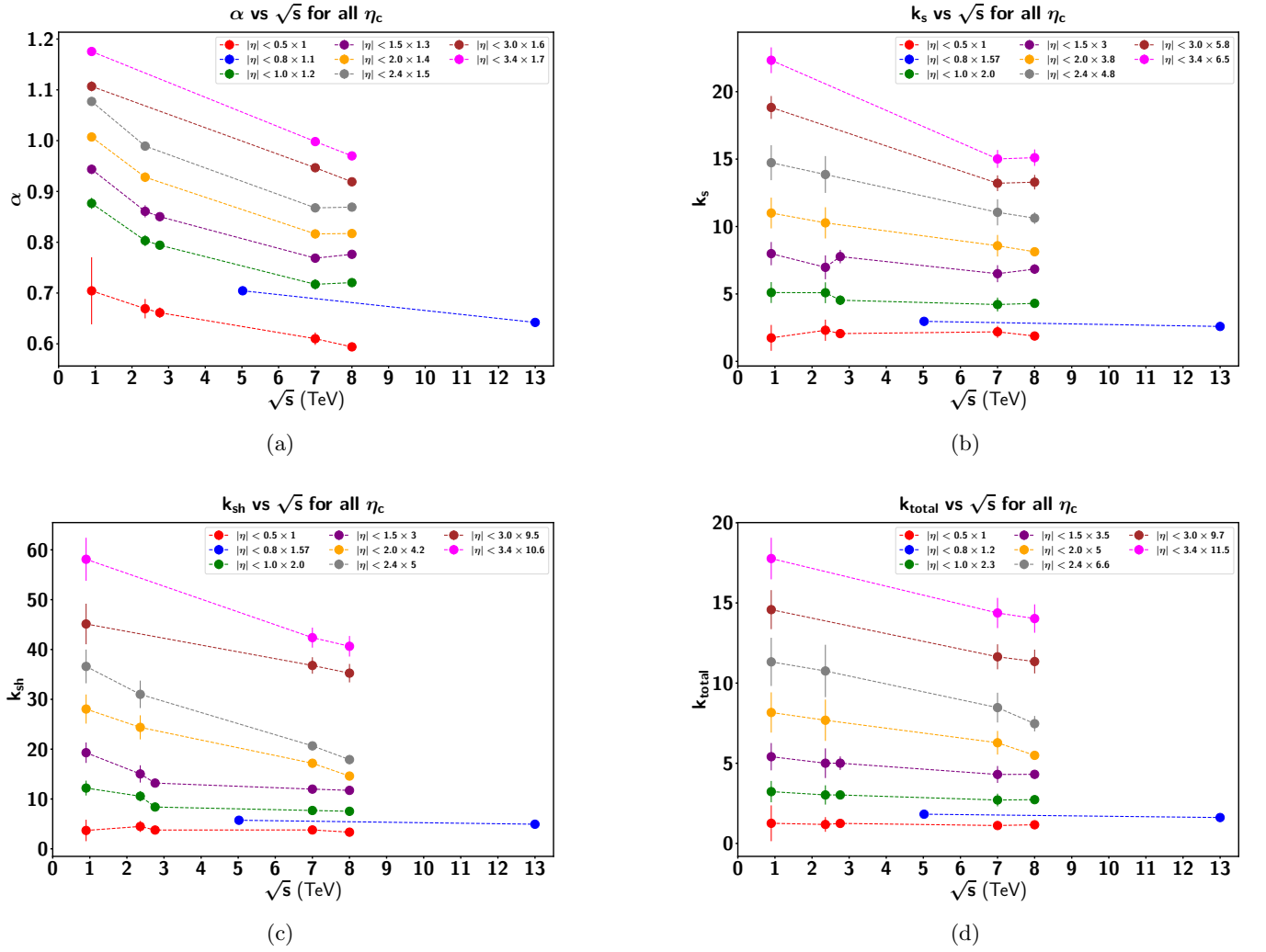


FIG. 4: Behavior of α , k_s , k_{sh} and k_{total} with increasing energy for various pseudorapidity windows ($-\eta_c < \eta < +\eta_c$). The lines are just to guide the eyes. The data points in blue refer to INEL events. All the others refer to NSD events.

- [10] A. Giovannini and R. Ugoccioni, Phys. Rev. D **59**, 094020 (1999); [erratum: Phys. Rev. D **69**, 059903 (2004)] [arXiv:hep-ph/9810446 [hep-ph]].
- [11] P. Ghosh, Phys. Rev. D **85**, 054017 (2012); [arXiv:1202.4221 [hep-ph]].
- [12] I. Zborovský, Eur. Phys. J. C **78**, 816 (2018); [arXiv:1811.11230 [hep-ph]].
- [13] A. Giovannini and R. Ugoccioni, Int. J. Mod. Phys. A **20**, 3897 (2005); [arXiv:hep-ph/0405251 [hep-ph]].
- [14] Z. Koba, H. B. Nielsen and P. Olesen, Nucl. Phys. B **40**, 317-334 (1972).
- [15] S. Acharya *et al.* [ALICE], Phys. Lett. B **845**, 138110 (2023); [arXiv:2211.15326 [nucl-ex]].
- [16] S. Acharya *et al.* [ALICE], Phys. Rev. D **108**, 072008 (2023); [arXiv:2211.15364 [nucl-ex]].
- [17] L. v. Gribov, E. m. Levin and M. g. Ryskin, Phys. Lett. B **121**, 65 (1983).
- [18] Y. V. Kovchegov and E. Levin, Camb. Monogr. Part. Phys. Nucl. Phys. Cosmol. **33**, 1 (2012), Oxford University Press, 2013, ISBN 978-1-009-29144-6, 978-1-009-29141-5, 978-1-009-29142-2, 978-0-521-11257-4, 978-1-139-55768-9, doi:10.1017/9781009291446.
- [19] H. M. Wang, J. F. Liu, Z. Y. Hou and X. J. Sun, Chin. Phys. C **37**, 084101 (2013); [arXiv:1305.5106 [nucl-th]].
- [20] D. Kharzeev, E. Levin and M. Nardi, Nucl. Phys. A **747**, 609 (2005); [arXiv:hep-ph/0408050 [hep-ph]].
- [21] K. J. Golec-Biernat and M. Wusthoff, Phys. Rev. D **59**, 014017 (1998); [arXiv:hep-ph/9807513 [hep-ph]].
- [22] K. Golec-Biernat and S. Sapeta, JHEP **03**, 102 (2018), [arXiv:1711.11360 [hep-ph]].
- [23] L. S. Moriggi, G. M. Peccini and M. V. T. Machado, Phys. Rev. D **102**, 034016 (2020); [arXiv:2005.07760 [hep-ph]].
- [24] C. Henkels, E. G. de Oliveira, R. Pasechnik and H. Trebien, Nucl. Phys. A **1055**, 123018 (2025); [arXiv:2310.06965 [hep-ph]].
- [25] F. Carvalho, F. O. Duraes, V. P. Goncalves and F. S. Navarra, Mod. Phys. Lett. A **23**, 2847 (2008).

η_c	data	\sqrt{s} (TeV)	λ	α	$\langle n \rangle_s$	$\langle n \rangle_{sh}$	$\langle n \rangle$	k_s	k_{sh}	k_{total}	χ^2/dof
0.5	[39]	0.90	0.895 ± 0.054	0.704 ± 0.066	2.803 ± 0.234	6.319 ± 1.270	3.437 ± 0.040	1.743 ± 0.960	3.685 ± 2.154	1.257 ± 1.117	0.265
		2.36	0.875 ± 0.039	0.669 ± 0.019	3.150 ± 0.182	8.719 ± 0.689	4.370 ± 0.050	2.310 ± 0.786	4.489 ± 1.099	1.183 ± 0.457	0.587
	[7]	2.76	0.936 ± 0.011	0.661 ± 0.010	3.028 ± 0.065	8.599 ± 0.273	4.599 ± 0.057	2.061 ± 0.336	3.770 ± 0.279	1.249 ± 0.168	0.057
	[39]	7.00	0.920 ± 0.032	0.610 ± 0.012	3.376 ± 0.182	11.214 ± 0.711	5.915 ± 0.075	2.192 ± 0.444	3.788 ± 0.232	1.117 ± 0.235	0.102
	[7]	8.00	0.955 ± 0.009	0.594 ± 0.008	3.270 ± 0.055	10.733 ± 0.219	6.018 ± 0.049	1.882 ± 0.263	3.344 ± 0.152	1.164 ± 0.108	0.106
0.8	[15]	5.02	1.072 ± 0.006	0.640 ± 0.002	4.195 ± 0.041	13.634 ± 0.130	8.135 ± 0.052	1.890 ± 0.054	3.652 ± 0.054	1.519 ± 0.073	0.615
		13.00	1.083 ± 0.005	0.584 ± 0.001	4.429 ± 0.041	16.763 ± 0.136	10.353 ± 0.064	1.650 ± 0.037	3.144 ± 0.026	1.346 ± 0.043	0.910
1.0	[39]	0.90	0.891 ± 0.021	0.730 ± 0.009	5.514 ± 0.176	14.160 ± 0.680	6.987 ± 0.081	2.552 ± 0.388	6.096 ± 0.745	1.405 ± 0.289	0.254
		2.36	0.893 ± 0.023	0.669 ± 0.009	6.310 ± 0.227	17.494 ± 0.808	8.938 ± 0.103	2.546 ± 0.386	5.280 ± 0.515	1.315 ± 0.261	0.355
	[7]	2.76	0.936 ± 0.009	0.662 ± 0.007	6.176 ± 0.122	17.594 ± 0.442	9.393 ± 0.116	2.268 ± 0.178	4.195 ± 0.190	1.315 ± 0.111	0.040
	[39]	7.00	0.918 ± 0.022	0.598 ± 0.008	6.994 ± 0.267	21.978 ± 0.943	11.958 ± 0.151	2.108 ± 0.258	3.847 ± 0.161	1.178 ± 0.172	0.113
	[7]	8.00	0.947 ± 0.008	0.600 ± 0.005	6.608 ± 0.104	22.196 ± 0.392	12.157 ± 0.098	2.151 ± 0.129	3.767 ± 0.109	1.187 ± 0.074	0.080
1.5	[39]	0.90	0.910 ± 0.016	0.726 ± 0.007	8.270 ± 0.212	20.798 ± 0.795	10.650 ± 0.124	2.663 ± 0.287	6.430 ± 0.684	1.546 ± 0.243	0.143
		2.36	0.925 ± 0.020	0.662 ± 0.009	9.427 ± 0.299	25.370 ± 1.044	13.704 ± 0.158	2.325 ± 0.295	5.010 ± 0.578	1.429 ± 0.264	0.180
	[7]	2.76	0.941 ± 0.008	0.654 ± 0.006	9.504 ± 0.177	26.216 ± 0.599	14.386 ± 0.177	2.590 ± 0.167	4.397 ± 0.220	1.430 ± 0.121	0.100
	[39]	7.00	0.918 ± 0.018	0.591 ± 0.007	10.723 ± 0.347	32.745 ± 1.153	18.097 ± 0.228	2.168 ± 0.211	3.994 ± 0.139	1.229 ± 0.151	0.188
	[7]	8.00	0.947 ± 0.007	0.597 ± 0.004	10.061 ± 0.142	33.238 ± 0.497	18.372 ± 0.149	2.281 ± 0.119	3.910 ± 0.112	1.231 ± 0.073	0.144
2.0	[39]	0.90	0.909 ± 0.015	0.719 ± 0.006	11.233 ± 0.269	27.433 ± 0.939	14.344 ± 0.167	2.895 ± 0.300	6.679 ± 0.696	1.633 ± 0.251	0.167
		2.36	0.929 ± 0.018	0.663 ± 0.007	12.671 ± 0.359	34.319 ± 1.193	18.543 ± 0.214	2.703 ± 0.305	5.804 ± 0.576	1.537 ± 0.258	0.191
		7.00	0.908 ± 0.016	0.583 ± 0.006	14.731 ± 0.447	43.493 ± 1.400	24.252 ± 0.306	2.257 ± 0.211	4.089 ± 0.146	1.256 ± 0.147	0.310
	[29]	8.00	0.898 ± 0.005	0.584 ± 0.004	14.539 ± 0.175	45.398 ± 0.526	24.580 ± 0.199	2.139 ± 0.065	3.478 ± 0.116	1.099 ± 0.053	0.861
2.4	[39]	0.90	0.913 ± 0.013	0.718 ± 0.005	13.464 ± 0.296	32.726 ± 1.001	17.245 ± 0.200	3.069 ± 0.270	7.321 ± 0.677	1.716 ± 0.228	0.180
		2.36	0.934 ± 0.016	0.660 ± 0.006	15.252 ± 0.394	40.810 ± 1.273	22.381 ± 0.258	2.887 ± 0.284	6.201 ± 0.551	1.630 ± 0.248	0.153
		7.00	0.907 ± 0.015	0.578 ± 0.006	17.846 ± 0.504	51.731 ± 1.520	29.133 ± 0.367	2.303 ± 0.202	4.132 ± 0.154	1.284 ± 0.141	0.411
	[29]	8.00	0.897 ± 0.007	0.579 ± 0.005	17.579 ± 0.255	53.966 ± 0.818	29.495 ± 0.239	2.213 ± 0.089	3.581 ± 0.179	1.132 ± 0.073	0.337
3.0	[29]	0.90	0.860 ± 0.006	0.692 ± 0.006	19.265 ± 0.303	41.306 ± 0.993	22.409 ± 0.253	3.247 ± 0.147	4.750 ± 0.428	1.503 ± 0.126	2.322
		7.00	0.912 ± 0.007	0.592 ± 0.004	21.332 ± 0.304	65.459 ± 0.960	35.886 ± 0.294	2.278 ± 0.101	3.873 ± 0.175	1.200 ± 0.080	0.281
		8.00	0.896 ± 0.007	0.574 ± 0.005	22.050 ± 0.313	66.437 ± 0.954	36.684 ± 0.297	2.291 ± 0.093	3.711 ± 0.195	1.170 ± 0.077	0.311
3.4	[29]	0.90	0.851 ± 0.006	0.691 ± 0.005	21.766 ± 0.321	46.526 ± 0.952	25.036 ± 0.283	3.435 ± 0.147	5.482 ± 0.407	1.545 ± 0.113	2.656
		7.00	0.916 ± 0.007	0.587 ± 0.004	24.058 ± 0.346	72.604 ± 1.059	40.405 ± 0.331	2.310 ± 0.102	3.998 ± 0.189	1.250 ± 0.082	0.216
		8.00	0.902 ± 0.007	0.571 ± 0.004	24.789 ± 0.344	73.676 ± 0.999	41.289 ± 0.334	2.324 ± 0.094	3.835 ± 0.195	1.220 ± 0.077	0.294

\sqrt{s} (TeV)	data	η_c	λ	α	$\langle n \rangle_s$	$\langle n \rangle_{sh}$	$\langle n \rangle$	k_s	k_{sh}	k_{total}	χ^2/dof
0.90	[39]	0.5	0.895 ± 0.054	0.704 ± 0.066	2.803 ± 0.234	6.319 ± 1.270	3.437 ± 0.040	1.743 ± 0.960	3.685 ± 2.154	1.257 ± 1.117	0.265
		1.0	0.891 ± 0.021	0.730 ± 0.009	5.514 ± 0.176	14.160 ± 0.680	6.987 ± 0.081	2.552 ± 0.388	6.096 ± 0.745	1.405 ± 0.289	0.254
		1.5	0.910 ± 0.016	0.726 ± 0.007	8.270 ± 0.212	20.798 ± 0.795	10.650 ± 0.124	2.663 ± 0.287	6.430 ± 0.684	1.546 ± 0.243	0.143
		2.0	0.909 ± 0.015	0.719 ± 0.006	11.233 ± 0.269	27.433 ± 0.939	14.344 ± 0.167	2.895 ± 0.300	6.679 ± 0.696	1.633 ± 0.251	0.167
		2.4	0.913 ± 0.013	0.718 ± 0.005	13.464 ± 0.296	32.726 ± 1.001	17.245 ± 0.200	3.069 ± 0.270	7.321 ± 0.677	1.716 ± 0.228	0.180
	[29]	3.0	0.860 ± 0.006	0.692 ± 0.006	19.265 ± 0.303	41.306 ± 0.993	22.409 ± 0.253	3.247 ± 0.147	4.750 ± 0.428	1.503 ± 0.126	2.322
		3.4	0.851 ± 0.006	0.691 ± 0.005	21.766 ± 0.321	46.526 ± 0.952	25.036 ± 0.283	3.435 ± 0.147	5.482 ± 0.407	1.545 ± 0.113	2.656
2.36	[39]	0.5	0.875 ± 0.039	0.669 ± 0.019	3.150 ± 0.182	8.719 ± 0.689	4.370 ± 0.050	2.310 ± 0.786	4.489 ± 1.099	1.183 ± 0.457	0.587
		1.0	0.893 ± 0.023	0.669 ± 0.009	6.310 ± 0.227	17.494 ± 0.808	8.938 ± 0.103	2.546 ± 0.386	5.280 ± 0.515	1.315 ± 0.261	0.355
		1.5	0.925 ± 0.020	0.662 ± 0.009	9.427 ± 0.299	25.370 ± 1.044	13.704 ± 0.158	2.325 ± 0.295	5.010 ± 0.578	1.429 ± 0.264	0.180
		2.0	0.929 ± 0.018	0.663 ± 0.007	12.671 ± 0.359	34.319 ± 1.193	18.543 ± 0.214	2.703 ± 0.305	5.804 ± 0.576	1.537 ± 0.258	0.191
		2.4	0.934 ± 0.016	0.660 ± 0.006	15.252 ± 0.394	40.810 ± 1.273	22.381 ± 0.258	2.887 ± 0.284	6.201 ± 0.551	1.630 ± 0.248	0.153
2.76	[7]	0.5	0.936 ± 0.011	0.661 ± 0.010	3.028 ± 0.065	8.599 ± 0.273	4.599 ± 0.057	2.061 ± 0.336	3.770 ± 0.279	1.249 ± 0.168	0.057
		1.0	0.936 ± 0.009	0.662 ± 0.007	6.176 ± 0.122	17.594 ± 0.442	9.393 ± 0.116	2.268 ± 0.178	4.195 ± 0.190	1.315 ± 0.111	0.040
		1.5	0.941 ± 0.008	0.654 ± 0.006	9.504 ± 0.177	26.216 ± 0.599	14.386 ± 0.177	2.590 ± 0.167	4.397 ± 0.220	1.430 ± 0.121	0.100
5.02	[15]	0.8	1.072 ± 0.006	0.640 ± 0.002	4.195 ± 0.041	13.634 ± 0.130	8.135 ± 0.052	1.890 ± 0.054	3.652 ± 0.054	1.519 ± 0.073	0.615
7.00	[39]	0.5	0.920 ± 0.032	0.610 ± 0.012	3.376 ± 0.182	11.214 ± 0.711	5.915 ± 0.075	2.192 ± 0.444	3.788 ± 0.232	1.117 ± 0.235	0.102
		1.0	0.918 ± 0.022	0.598 ± 0.008	6.994 ± 0.267	21.978 ± 0.943	11.958 ± 0.151	2.108 ± 0.258	3.847 ± 0.161	1.178 ± 0.172	0.113
		1.5	0.918 ± 0.018	0.591 ± 0.007	10.723 ± 0.347	32.745 ± 1.153	18.097 ± 0.228	2.168 ± 0.211	3.994 ± 0.139	1.229 ± 0.151	0.188
		2.0	0.908 ± 0.016	0.583 ± 0.006	14.731 ± 0.447	43.493 ± 1.400	24.252 ± 0.306	2.257 ± 0.211	4.089 ± 0.146	1.256 ± 0.147	0.310
		2.4	0.907 ± 0.015	0.578 ± 0.006	17.846 ± 0.504	51.731 ± 1.520	29.133 ± 0.367	2.303 ± 0.202	4.132 ± 0.154	1.284 ± 0.141	0.411
	[29]	3.0	0.912 ± 0.007	0.592 ± 0.004	21.332 ± 0.304	65.459 ± 0.960	35.886 ± 0.294	2.278 ± 0.101	3.873 ± 0.175	1.200 ± 0.080	0.281
		3.4	0.916 ± 0.007	0.587 ± 0.004	24.058 ± 0.346	72.604 ± 1.059	40.405 ± 0.331	2.310 ± 0.102	3.998 ± 0.189	1.250 ± 0.082	0.216
8.00	[7]	0.5	0.955 ± 0.009	0.594 ± 0.008	3.270 ± 0.055	10.733 ± 0.219	6.018 ± 0.049	1.882 ± 0.263	3.344 ± 0.152	1.164 ± 0.108	0.106
		1.0	0.947 ± 0.008	0.600 ± 0.005	6.608 ± 0.104	22.196 ± 0.392	12.157 ± 0.098	2.151 ± 0.129	3.767 ± 0.109	1.187 ± 0.074	0.080
		1.5	0.947 ± 0.007	0.597 ± 0.004	10.061 ± 0.142	33.238 ± 0.497	18.372 ± 0.149	2.281 ± 0.119	3.910 ± 0.112	1.231 ± 0.073	0.144
	[29]	2.0	0.898 ± 0.005	0.584 ± 0.004	14.539 ± 0.175	45.398 ± 0.526	24.580 ± 0.199	2.139 ± 0.065	3.478 ± 0.116	1.099 ± 0.053	0.861
		2.4	0.897 ± 0.007	0.579 ± 0.005	17.579 ± 0.255	53.966 ± 0.818	29.495 ± 0.239	2.213 ± 0.089	3.581 ± 0.179	1.132 ± 0.073	0.337
		3.0	0.896 ± 0.007	0.574 ± 0.005	22.050 ± 0.313	66.437 ± 0.954	36.684 ± 0.297	2.291 ± 0.093	3.711 ± 0.195	1.170 ± 0.077	0.311
		3.4	0.902 ± 0.007	0.571 ± 0.004	24.789 ± 0.344	73.676 ± 0.999	41.289 ± 0.334	2.324 ± 0.094	3.835 ± 0.195	1.220 ± 0.077	0.294
13.00	[15]	0.8	1.083 ± 0.005	0.584 ± 0.001	4.429 ± 0.041	16.763 ± 0.136	10.353 ± 0.064	1.650 ± 0.037	3.144 ± 0.026	1.346 ± 0.043	0.910

- [27] X. P. Duan, L. Chen, G. L. Ma, C. A. Salgado and B. Wu, [arXiv:2503.24200 [hep-ph]].
- [28] A. Giovannini and R. Ugoccioni, Nucl. Phys. B Proc. Suppl. **71**, 201 (1999); [arXiv:hep-ph/9710361 [hep-ph]].
- [29] S. Acharya *et al.* [ALICE], Eur. Phys. J. C **77**, 852 (2017); [arXiv:1708.01435 [hep-ex]].
- [30] V. V. Begun, M. Gazdzicki and M. I. Gorenstein, Phys. Rev. C **78**, 024904 (2008); [arXiv:0804.0075 [hep-ph]].
- [31] M. Maćkowiak-Pawłowska *et al.* [NA61/SHINE], J. Phys. Conf. Ser. **509**, 012044 (2014); [arXiv:1402.0707 [hep-ex]].
- [32] A. Chandra, B. Ali and S. Ahmad, Adv. High Energy Phys. **2019**, 3905376 (2019); [arXiv:1908.00233 [nucl-th]].
- [33] G. R. Germano and F. S. Navarra, Phys. Rev. D **105**, 014005 (2022); [arXiv:2110.12028 [hep-ph]].
- [34] L. S. Moriggi, F. S. Navarra and M. V. T. Machado, [arXiv:2506.09899 [hep-ph]].
- [35] V. Khachatryan *et al.* [CMS], JHEP **02**, 041 (2010); [arXiv:1002.0621 [hep-ex]].
- [36] V. Khachatryan *et al.* [CMS], Phys. Rev. Lett. **105**, 022002 (2010); [arXiv:1005.3299 [hep-ex]].
- [37] M. Broilo, D. A. Fagundes, E. G. S. Luna and M. J. Menon, Phys. Lett. B **799**, 135047 (2019); [arXiv:1904.10061 [hep-ph]].
- [38] T. V. Iser and E. G. S. Luna, Acta Phys. Polon. Supp. **18**, 1-A42 (2025); [arXiv:2502.03168 [hep-ph]].
- [39] V. Khachatryan *et al.* [CMS], JHEP **01**, 079 (2011); [arXiv:1011.5531 [hep-ex]].
- [40] A. Giovannini and R. Ugoccioni, Phys. Rev. D **60**, 074027 (1999); [arXiv:hep-ph/9905210 [hep-ph]].